Ion selectivities of the Ca^{2+} sensors for exocytosis in rat phaeochromocytoma cells

Takuya Kishimoto*†, Ting-Ting Liu*†, Yasunori Ninomiya†, Hiroshi Takagi‡, Tohru Yoshioka‡, Graham C. R. Ellis-Davies§, Yasushi Miyashita*† and Haruo Kasai*

*Department of Cell Physiology, National Institute for Physiological Sciences, Okazaki 444-8585, †Department of Physiology, University of Tokyo School of Medicine, Bunkyo-ku, Tokyo 113-0033, ‡Department of Molecular Neurosciences, Waseda University, Mikajima, Saitama 359-1192, Japan and §Department of Pharmacology and Physiology, MCP Hahnemann University, Philadelphia, PA 19129, USA

(Received 7 December 2000; accepted after revision 30 January 2001)

1. The ion selectivities of the Ca^{2+} sensors for the two components of exocytosis in rat phaeochromocytoma (PC12) cells were examined by measurement of membrane capacitance and amperometry. The cytosolic concentrations of metal ions were increased by photolysis of caged-Ca^{2+} compounds and measured with low-affinity indicators benzothiazole coumarin (BTC) or 5-nitrobenzothiazole coumarin (BTC-5N).

2. The Ca^{2+}-induced increases in membrane capacitance comprised two phases with time constants of 30–100 ms and 5 s. Amperometric events reflecting the exocytosis of large dense-core vesicles occurred selectively in the slow phase, even with increases in the cytosolic Ca^{2+} concentration of > 0.1 mM.

3. The slow component of exocytosis was activated by all metal ions investigated, including Cd^{2+} (median effective concentration, 18 pM), Mn^{2+} (500 nM), Co^{2+} (900 nM), Ca^{2+} (8 μM), Sr^{2+} (180 μM), Ba^{2+} (280 μM) and Mg^{2+} (> 5 mM). In contrast, the fast component of exocytosis was activated by Cd^{2+} (26 pM), Mn^{2+} (620 nM), Ca^{2+} (24 μM) and Sr^{2+} (320 μM), but was only slightly increased by Ba^{2+} (> 2 mM) and Co^{2+} and not at all by Mg^{2+}.

4. The fast component, but not the slow component, was competitively blocked by Na^+ (median effective concentration, 44 mM) but not by Li^+, K^+ or Cs^+. Thus, the Ca^{2+} sensor for the fast component of exocytosis is more selective than is that for the slow component; moreover, this selectivity appears to be based on ionic radius, with cations with radii of 0.84 to 1.13 Å (1 Å = 0.1 nm) being effective.

5. These data support a role for synaptotagmin–phospholipid as the Ca^{2+} sensor for the exocytosis of large dense-core vesicles and they suggest that an additional Ca^{2+}-sensing mechanism operates in the synchronous exocytosis of synaptic-like vesicles.

Regulated secretion in neurosecretory cells is mediated by two types of organelles, large dense-core vesicles (LVs) and small synaptic-like vesicles (SVs), that differ in their biogenesis and contents (Clift *et al.* 1990; Kelly, 1993; Itakura *et al.* 1999). The exocytoses of both LVs and SVs exhibit distinct ion selectivities. Exocytosis of LVs from endocrine cells is supported when external Ca^{2+} is replaced with Ba^{2+} (Berggren, 1981; Douglas *et al.* 1983; Brown *et al.* 1990; von Ruden *et al.* 1993; Seward *et al.* 1996; Borges *et al.* 1997; Nucifora & Fox, 1998). In contrast, synchronous SV exocytosis from presynaptic terminals is not maintained by Ba^{2+} in the external solution (Dodge *et al.* 1969; Alvarez-Leefmans *et al.* 1978; Augustine & Eckert, 1984; Medina *et al.* 1994; but see Ohno-Shosaku *et al.* 1994), although Ba^{2+} does support asynchronous slow neurotransmitter release (Silinsky, 1978; McMahon & Nicholls, 1993; Sihra *et al.* 1993; Verhage *et al.* 1995). None of these studies, however, examined the effects of divalent cations introduced directly into the cytosol.

The LVs and SVs of rat phaeochromocytoma (PC12) cells contain monoamines and acetylcholine, respectively (Greene & Tischler, 1976; Baumert *et al.* 1990; Schmidt *et al.* 1997). We have previously shown that abrupt increases in the cytosolic Ca^{2+} concentration ($[Ca^{2+}]_i$) generated by photolysis of caged-Ca^{2+} compounds trigger

Table 1. Internal solutions

Solution	Na_4-DM-nitrophen (mM)	Monovalent cation glutamate (mM)	pH buffer (mM)	Monovalent cation chloride (mM)	Divalent cation chloride (mM)	Ca^{2+} indicator (mM)
Sol-Ca	10–20	100 Cs-glutamate	50 Cs-Hepes	5 CsCl	4–11 $CaCl_2$	0.2 BTC or BTC-5N
Sol-Sr	10	100 Cs-glutamate	50 Cs-Hepes	5 CsCl	4 $SrCl_2$	0.2 BTC
Sol-Ba	10–20	100 Cs-glutamate	50 Cs-Hepes	5 CsCl	4–8 $BaCl_2$	0.2 BTC or BTC-5N
Sol-Cd	10	100 Cs-glutamate	50 Cs-Hepes	5 CsCl	4 $CdCl_2$	0.2 BTC
Sol-Mn	10	100 Cs-glutamate	50 Cs-Hepes	5 CsCl	4 $MnCl_2$	0.2 BTC
Sol-Co	10–20	100 Cs-glutamate	50 Cs-Hepes	5 CsCl	4–9 $CoCl_2$	0.2 BTC or BTC-5N
Sol-Mg	10	100 Cs-glutamate	50 Cs-Hepes	5 CsCl	5 $MgCl_2$	0.2 BTC
Sol-Cs	10	100 Cs-glutamate	50 Cs-Hepes	5 CsCl	4 $CaCl_2$	0.2 BTC
Sol-Li	10	100 Li-glutamate	50 Li-Hepes	5 LiCl	4 $CaCl_2$	0.2 BTC
Sol-K	10	100 K-glutamate	50 K-Hepes	5 KCl	4 $CaCl_2$	0.2 BTC
Sol-Na	10	100 Na-glutamate	50 Na-Hepes	5 NaCl	4 $CaCl_2$	0.2 BTC

The pH and osmolarity of all internal solutions were adjusted to 7.4 and between 290 to 310 mosmol l^{-1}, respectively.

two components of exocytosis in PC12 cells with markedly different time constants of 30–100 ms and 10 s (Kasai *et al.* 1996). The slow component appears to be mediated by LVs, given that it is accompanied by monoamine secretion; conversely, the fast component is probably mediated by SVs, given that it is associated with secretion of acetylcholine, but not with that of monoamines (Ninomiya *et al.* 1997). Dissociation of the fast increase in membrane capacitance (C_m) from the amperometric detection of monoamine secretion has also been demonstrated in pancreatic β cells (Takahashi *et al.* 1997) and adrenal chromaffin cells (Ninomiya *et al.* 1997; Haller *et al.* 1998; Kasai, 1999). This dissociation is less marked in chromaffin cells (Ninomiya *et al.* 1997) and most increases in C_m in these cells at $[Ca^{2+}]_i$ values of < 100 μM have been attributed to the exocytosis of LVs (Haller *et al.* 1998).

To characterise the ion selectivities of exocytosis of LVs and SVs, we have chosen to study PC12 cells, because of the pronounced differences in the corresponding time courses of exocytosis. We triggered exocytosis by inducing the photolysis of caged-Ca^{2+} compounds loaded with various metal ions, which results in direct increases in the cytosolic concentrations of these ions, and we monitored exocytosis by measurement of C_m and amperometry. We detected marked differences in ion selectivity between exocytosis of LVs and that of SVs and these selectivities are similar to those of endocrine secretion and synchronous synaptic neurotransmitter release, respectively. The ion selectivities of exocytosis in PC12 cells support a role for synaptotagmin–phospholipid as the Ca^{2+} sensor (Brose *et al.* 1992; Bommert *et al.* 1993; Elferink *et al.* 1993; Südhof & Rizo, 1996; Thomas & Elferink, 1998; Mikoshiba *et al.* 1999) for the exocytosis of LVs, but they suggest an additional mechanism for the Ca^{2+}-dependent exocytosis of SVs.

METHODS

Preparation of cells

For most experiments, we used a subclone (B7) of PC12 cells kindly provided by K. Inoue (NIHS, Tokyo, Japan) (47th passage from the original PC12 clone; Greene & Tischler, 1976). The cells were grown in Dulbecco's modified Eagle's medium (DMEM) supplemented with 7 % horse serum, 7 % fetal bovine serum and 50 μg ml^{-1} penicillin (in the absence of nerve growth factor) and were maintained at 37 °C under an atmosphere of 10 % CO_2 (Kasai *et al.* 1996). They were passaged approximately once a week and plated 1–3 days before patch-clamp experiments on circular cover glasses (diameter, 14 mm; Matsunami Glass, Osaka, Japan) that had been coated with poly-L-lysine (10 μg ml^{-1}) (Sigma) for 30 min and placed in four-well culture plates. All electrophysiological experiments were performed at 20–24 °C.

Amperometric detection of monoamine secretion

Oxidative currents due to monoamines were recorded with a patch-clamp amplifier (CEZ2400; Nihon Kohden, Tokyo, Japan) and a carbon-fibre electrode (Pro-CFE; Dagan, Minneapolis, MN, USA) with an applied positive potential (650 mV). Amperometric currents were filtered at 40 Hz and sampled at 83 Hz. Artifacts of amperometry due to flash irradiation were subtracted with the use of a trace from the same cell at a second or third flash for which no secretion was detected. In the amperometric latency histogram, the onset of the current spike was taken as the time at which the transient current became increased by twice the size of the standard deviation of the baseline noise level.

Capacitance measurement

Capacitance was measured in cells patch clamped in the whole-cell mode as described previously (Kasai *et al.* 1996). The external solution (pH 7.4, 310 mosmol l^{-1}) contained (mM): 140 NaCl, 5 KCl, 2 $CaCl_2$, 1 $MgCl_2$, 10 Hepes-NaOH and 10 glucose. For Ca^{2+} jump experiments, the patch pipette contained Sol-Ca solution (Table 1), which comprised (mM): 100 caesium glutamate, 5 CsCl and 50 Hepes-CsOH (pH 7.4); the solution also contained 0.2 mM benzothiazole coumarin (BTC) or 5-nitrobenzothiazole coumarin (BTC-5N) (Molecular Probes, Eugene, OR, USA) for a low-affinity or very-low-affinity Ca^{2+} indicator, respectively, as well as 10–20 mM dimethoxy-nitrophenamine tetrasodium salt (DM-nitrophen) (Calbiochem, La Jolla, CA, USA) or dimethoxynitrophenyl-EGTA-4 (DMNPE-4) (Ellis-Davies, 1998), as caged-Ca^{2+} compounds, together with 4–11 mM

Table 2. Calibration parameters of BTC and BTC-5N for various divalent cations

Divalent cation	BTC				BTC-5N			
	K_d'	R_{max}	K_d	F_{min}/F_{max}	K_d'	R_{max}	K_d	F_{min}/F_{max}
Ca^{2+}	102 μM	2.5	—	—	4.4 mM	1.2	—	—
Sr^{2+}	1.32 mM	1.6	—	—	—	—	—	—
Ba^{2+}	227 μM	4.7	—	—	3.6 mM	2.2	—	—
Cd^{2+}	168 pM	3.2	—	—	—	—	—	—
Mn^{2+}	—	—	0.30 μM	0.208	—	—	—	—
Co^{2+}	—	—	1.0 μM	0.256	—	—	512 μM	0.102

R_{min} and R_{max} represent the fluorescence ratios of metal-free and metal-bound BTC (or BTC-5N), respectively, and K_d' is the apparent dissociation constant. F_{min}/F_{max} indicates the maximal value of quenching by the metal ion and K_d is the dissociation constant.

$CaCl_2$. To induce concentration jumps of other metal ions, we replaced $CaCl_2$ with the corresponding chloride salt (Sol-Ba, Sol-Sr, Sol-Cd, Sol-Mn, Sol-Co and Sol-Mg in Table 1). In the experiments shown in Figs 5 and 6, all internal Cs^+ (115 mM) was replaced with Na^+, K^+ or Li^+ (Sol-Na, Sol-K and Sol-Li in Table 1). If necessary, the pH of the solutions was readjusted with HCl and the osmolarity of the internal solution was adjusted to between 290 and 310 mosmol l^{-1}.

For measurement of membrane capacitance, a 1 kHz sine-wave voltage command with a peak-to-peak amplitude of 100 mV was superimposed on the holding potential of −20 mV. The C_m was calculated from 10 cycles of sine waves and was sampled at 83 Hz. The influx of Ca^{2+} through voltage-gated Ca^{2+} channels contributed little to exocytosis under our experimental conditions, given that the cytosolic concentrations of divalent cations were clamped with high concentrations of caged-Ca^{2+} compounds. Large increases in the concentrations of divalent cations might be expected to trigger Ca^{2+} release from cytosolic Ca^{2+} binding sites (Tomsig & Suszkiw, 1996). However, such Ca^{2+} release is likely to be negligible under our experimental conditions because the cytosol was perfused with high concentrations of caged-Ca^{2+} compound with a dissociation constant (K_d) for Ca^{2+} of 5 nM. If we assume that 5 nM free Ca^{2+} might remain in the cytosol, then the total concentration of bound Ca^{2+} would be predicted to be < 1 μM (assuming a binding ratio of 100) (Maeda *et al.* 1999). Such small increases in $[Ca^{2+}]_i$ caused little exocytosis (Fig. 1).

The C_m of PC12-B7 cells (Kasai *et al.* 1996; Ninomiya *et al.* 1997) was 7.3 ± 2.7 pF (mean ± S.D.; $n = 201$). Mean access resistance was 8.9 ± 3.9 MΩ. Vertical and horizontal error bars in figures represent S.E.M. and S.D., respectively. Continuous curves on graphs represent the best fit of the data obtained with the use of the Hill equation, with a Hill coefficient of 3.

Photolysis of caged-Ca^{2+} compounds

Photolysis of DM-nitrophen or DMNPE-4 was induced with a xenon flash lamp (High Tech Instrument, Aberdeen, UK) for Ca^{2+}, Sr^{2+}, Ba^{2+} and Cd^{2+}. A mercury lamp (IX-RFC; Olympus, Tokyo) was used for Mn^{2+}, Co^{2+} and Mg^{2+}, because the caged compounds were resistant to photolysis in these metal-bound forms. The radiation of the mercury lamp was gated through an electronic shutter (Copal, Tokyo) with an opening duration of 33–125 ms.

Measurement of divalent cation concentration

The cytosolic concentrations of Ca^{2+}, Sr^{2+}, Ba^{2+} and Cd^{2+} were measured as described (Grynkiewicz *et al.* 1985) with the use of the ratiometric long-wavelength indicator BTC; large concentrations of Ca^{2+} or Ba^{2+} were measured with BTC-5N. BTC or BTC-5N was excited with light emitted from a xenon lamp (TILL Photonics, Planegg, Germany) alternating rapidly between 430 and 480 nm, and the emitted fluorescence was collected through the objective lens, passed through an LP520 filter and detected with a photomultiplier (NT5783; Hamamatsu Photonics, Hamamatsu City, Japan). The cytosolic concentration of each metal ion ($[M^{2+}]_i$) was estimated from the fluorescence ratio ($R = F_{430}/F_{480}$) as:

$$[M^{2+}]_i = K_d'(R - R_{min})/(R_{max} - R),$$

where K_d' represents the apparent dissociation constant for the indicator and R_{min} and R_{max} are the fluorescence ratios of metal-free and metal-bound BTC (or BTC-5N), respectively (Grynkiewicz *et al.* 1985). The calibration parameters were experimentally obtained as described below and are shown in Table 2. The measurement of $[M^{2+}]_i$ was performed at 83 Hz and the mean values during every 3 s are presented (Figs 1–4).

The cytosolic concentrations of Mn^{2+} and Co^{2+} were measured on the basis of quenching by the metal ions of BTC fluorescence excited at 480 nm; BTC-5N was used for determination of large concentrations of Co^{2+}. The concentration of Co^{2+} or Mn^{2+} was estimated from the fluorescence value obtained during stimulation (F) and that obtained before stimulation (F_0) according to the equation:

$$[M^{2+}]_i = K_d(1 - F/F_0)/(F/F_0 - F_{min}/F_{max}),$$

where K_d represents the dissociation constant and F_{min}/F_{max} is the ratio of the fluorescence of the metal-bound quenched dye to that of the free dye. The calibration parameters for Co^{2+} and Mn^{2+} were obtained experimentally as described below and are shown in Table 2. The cytosolic concentration of Mg^{2+} was estimated by assuming both the dissociation constant of photolysed DM-nitrophen to be 6 mM (Delaney & Zucker, 1990) and no cytosolic binding of Mg^{2+}.

Estimation of calibration parameters of BTC and BTC-5N

The K_d' values of BTC and BTC-5N were measured with an internal solution from which trace metal ions were removed by BAPTA polystyrene (Calcium Sponge S; Molecular Probes). The fluorescence of BTC or BTC-5N was measured with a spectrofluorimeter (FP-777; JASCO, Tokyo) at excitation wavelengths of 430 and 480 nm and emission wavelengths of 510 and 530 nm, respectively. The fluorescence ratios of BTC and BTC-5N in the absence of any divalent cations (R_{min}) were 0.61 and 0.57, respectively, and the R_{max} values were measured in the presence of 10 mM cation. To obtain the K_d' values of BTC and BTC-5N for Ca^{2+}, Sr^{2+} or Ba^{2+}, we measured the fluorescence ratios of 1 μM BTC or 10 μM BTC-5N in the presence of various concentrations of added divalent cation (> 100 μM), given that K_d' values of BTC or BTC-5N for these cations are > 100 μM. The values are summarized in Table 2.

The K_d' value of BTC for Cd^{2+} and the K_d values of BTC and BTC-5N for Co^{2+} or Mn^{2+} were estimated with solutions in which the

concentrations of metal ions were adjusted with chelators in the presence of 1 μM BTC or BTC-5N. For the buffering of Cd^{2+}, Mn^{2+} and Co^{2+}, we used 10 mM EDTA-OH, 1,3-diamino-2-hydroxypropane-*N*,*N*,*N*′*N*′-tetraacetic acid (DPTA-OH) and *N*,*N*-bis(2-hydroxyethyl)glycine (DHEG), respectively. The values thus obtained are listed in Table 2. The affinities of the buffers at pH 7.4 were estimated from previously determined pK_a (−log of the dissociation constant) values of chelators (9.86, 9.46 and 8.14 for EDTA-OH, DPTA-OH and DHEG, respectively) and from the stability constants of metal ions (5.31 for EDTA-OH and Cd^{2+}, 6.96 for DPTA-OH and Mn^{2+} and 8.14 for DHEG and Co^{2+}) as 7.31 pM for EDTA-OH and Cd^{2+}, 0.137 μM for DPTA-OH and Mn^{2+} and 6.1 μM for DHEG and Co^{2+} (Martell & Smith, 1974).

Values of K_d' may vary depending on the setup for measurement because of differences in the intensities and spectra of excitation lights. We applied the K_d' values obtained with the spectrometer to those of the patch-clamp setup, given that the determined K_d' value of BTC for Ca^{2+} was ~100 μM with both setups.

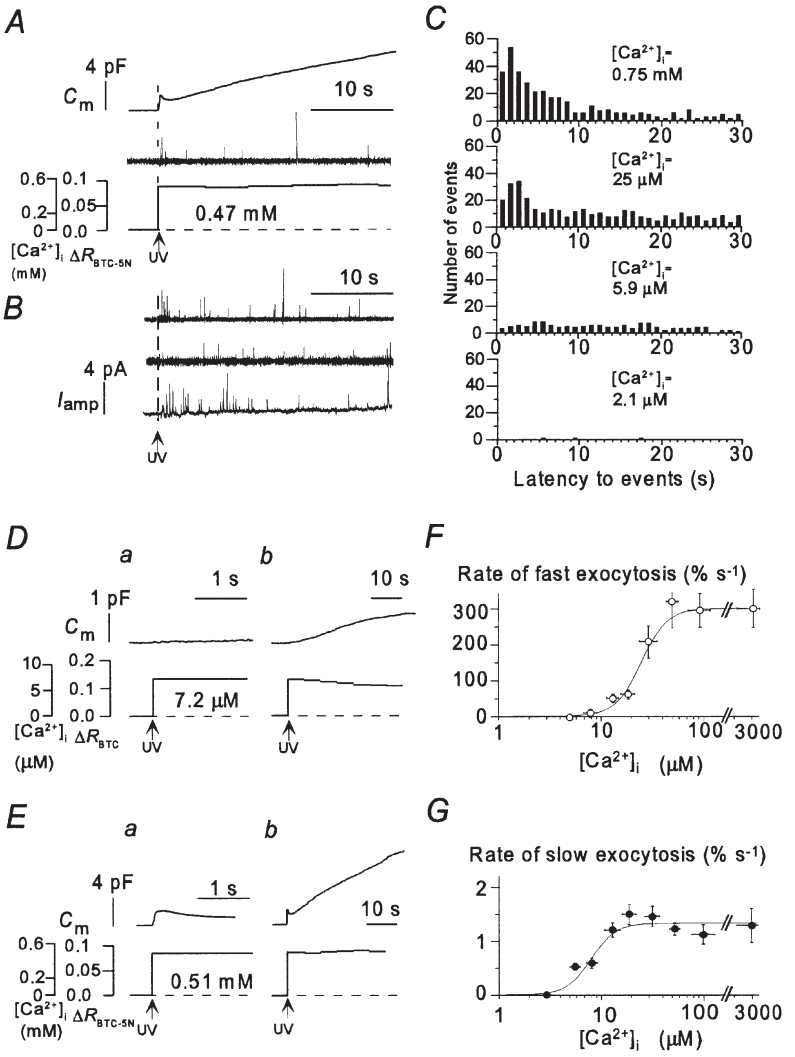

Figure 1. Ca^{2+}-induced exocytosis

A, time course of exocytosis in a PC12 cell during a Ca^{2+} jump to 0.47 mM. The changes in C_m, amperometric current, as well as $[Ca^{2+}]_i$ and ΔR for BTC-5N recorded from the same cell are shown in the upper, middle and lower traces, respectively. The time of photolysis of the caged-Ca^{2+} compound is indicated by UV (ultraviolet). *B*, three examples of amperometric current (I_{amp}) recorded during large Ca^{2+} jumps (> 0.1 mM). Each spike reflects quantal secretion of monoamines. *C*, latency distribution of quantal monoamine secretion. Data were obtained during four different Ca^{2+} jumps (mean ± S.D.: 750 ± 520, 25 ± 8.0, 5.9 ± 2.1 and 2.1 ± 1.0 μM, respectively) in 8–20 cells. The latency was defined as the time between the onset of the Ca^{2+} jump and that of the quantal event. *D* and *E*, two components of Ca^{2+}-dependent exocytosis. Representative experiments are shown for two different cells. Changes in C_m and the time courses of $[Ca^{2+}]_i$ and ΔR for either BTC (*D*) or BTC-5N (*E*) are shown in the upper and lower traces, respectively. The time axis in traces *a* is expanded by a factor of > 20 relative to that in traces *b*. *F* and *G*, dependence on $[Ca^{2+}]_i$ of the peak rates of the fast and slow components of exocytosis, respectively. Each point is the mean value from 4–9 experiments performed with different cells and with pipette solutions containing DM-nitrophen or DMNPE-4 loaded with various amounts of $CaCl_2$.

RESULTS

Two components of Ca^{2+}-dependent exocytosis in PC12 cells

Increases in $[Ca^{2+}]_i$ of > 10 μM generated in PC12 cells by photolysis of caged-Ca^{2+} compounds result in a two-phase increase in C_m (Kasai *et al.* 1996, 1999) (Fig. 1*A*, *D* and *E*). The time derivatives of capacitance traces exhibited two peaks, representing the release rates of the two different components of Ca^{2+}-dependent exocytosis (Kasai *et al.* 1996). The fast component of the increase in C_m in PC12 cells probably represents synchronous exocytosis of SVs (Ninomiya *et al.* 1997; Kasai, 1999), because little exocytosis of monoamines was detected at such early times (Fig. 1*B* and *C*). We quantified the rate of synchronous SV exocytosis from the maximal slope of the increase in C_m apparent within 1 s. The peak value actually appeared within 0.2 s after the Ca^{2+} jump in most experiments and was not much affected by endocytosis, which occurred after a longer delay (Fig. 1*Ea*) (Smith & Betz, 1996). The slow component of the increase in C_m probably represents exocytosis of LVs, given that its time course (Fig. 1*A–C*) and Ca^{2+} dependence (Fig. 1*C* and *G*) were identical to those of quantal monoamine secretion. We therefore quantified the rate of LV exocytosis from the maximal slope of the increase in C_m apparent after 1 s. The peak release rates were normalized to the total membrane area of each cell and are expressed in units of per cent per second (% s^{-1}) and plotted against peak $[Ca^{2+}]_i$ in Fig. 1*F* and *G*.

The rate of the slow component of exocytosis in PC12 cells is less than one-tenth that of quantal monoamine secretion in chromaffin cells (Ninomiya *et al.* 1997) and the rate of the fast component of exocytosis in PC12 cells is smaller than that of neurotransmitter release from synapses by a factor of 200 (Bollman *et al.* 2000; Schneggenburger & Neher, 2000). To examine whether the measured slow rates of exocytosis in PC12 cells were due to the relatively small values of $[Ca^{2+}]_i$ achieved in our previous studies (Kasai *et al.* 1996; Ninomiya *et al.* 1997), we applied larger increases in $[Ca^{2+}]_i$ with the use

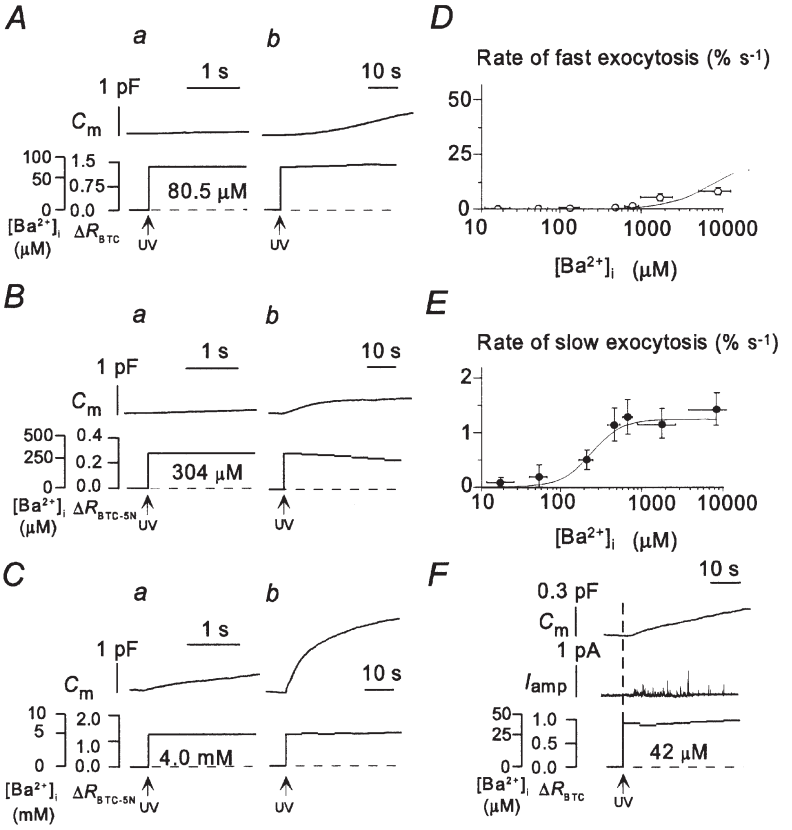

Figure 2. Ba^{2+}-induced exocytosis

A–C, representative examples of the time course of Ba^{2+}-dependent exocytosis in three different PC12 cells. Changes in C_m as well as in $[Ba^{2+}]_i$ and ΔR for BTC (*A*) or BTC-5N (*B* and *C*) are shown in the upper and lower traces, respectively. The time axis in traces *a* is expanded by a factor of > 20 compared with that in traces *b*. *D* and *E*, dependence on $[Ba^{2+}]_i$ of the peak rates of the fast and slow components of exocytosis, respectively. Each point is the mean value from 3–10 experiments performed with different cells and with pipette solutions containing DM-nitrophen or DMNPE-4 loaded with various amounts of $BaCl_2$. *F*, example of amperometric current recorded over a period of 30 s during a Ba^{2+} jump to 42 μM.

of DM-nitrophen or DMNPE-4 loaded with higher concentrations of $CaCl_2$. Measurement of $[Ca^{2+}]_i$ was also performed with BTC-5N, whose affinity for Ca^{2+} is lower than that of BTC. The mean values for the maximal rates of the slow and fast components of exocytosis were 1.39 ± 0.64 and $301 \pm 67\,\% \,s^{-1}$ even when the applied increases in $[Ca^{2+}]_i$ were > 0.1 mM (Fig. 1*A* and *B*); these values are not substantially larger than those achieved at 50 μM (Fig. 1*F* and *G*) (Kasai *et al.* 1996). Consistent with our previous results, the slow component of the increase in C_m occurred at the same time as did quantal monoamine secretion (Fig. 1*A–C*) and exhibited a similar dependence on Ca^{2+}. No rapid monoamine secretion was detected even at $[Ca^{2+}]_i$ values of > 0.1 mM. Thus, we confirmed that the half-maximal rates for the slow and fast components of exocytosis were attained at $[Ca^{2+}]_i$ values of 8 and 24 μM, respectively, with Hill coefficients of 3 (Fig. 1*F* and *G*). Cooperativity in the action of Ca^{2+} on exocytosis has been demonstrated both in endocrine cells (Knight & Baker, 1982) and in presynaptic terminals (Dodge & Rahamimoff, 1967; Augustine & Charlton, 1986; Takahashi & Momiyama, 1993).

Sensitivities of the two components of exocytosis to Ba^{2+} and Sr^{2+}

With the use of the same techniques, we examined the selectivities of exocytosis of LVs and SVs to the alkaline earth metal ions Ba^{2+} and Sr^{2+}. We found that Ba^{2+} selectively triggered the slow component of exocytosis at concentrations of < 1 mM. The slow component was induced at $[Ba^{2+}]_i$ values of > 30 μM, the half-maximal release rate was attained at 280 μM and the maximal rate ($1.23 \pm 0.3\,\% \,s^{-1}$) was achieved at 400 μM (Fig. 2*A*, *B* and *E*). The Ba^{2+}-induced monoamine secretion occurred in parallel with the slow component of the increase in C_m (Fig. 2*F*). The maximal rate of the Ba^{2+}-induced slow component was the same as that of the slow component of Ca^{2+}-induced exocytosis (Figs 1*G* and 2*E*). With increases in $[Ba^{2+}]_i$ of > 2 mM, we occasionally detected the fast component of exocytosis, but the rate ($> 8.1 \pm 2.2\,\% \,s^{-1}$) was less than one-twentieth of that of the corresponding value for Ca^{2+} jumps (Fig. 2*C* and *D*). Thus, Ba^{2+} induces synchronous SV exocytosis only at very high concentrations.

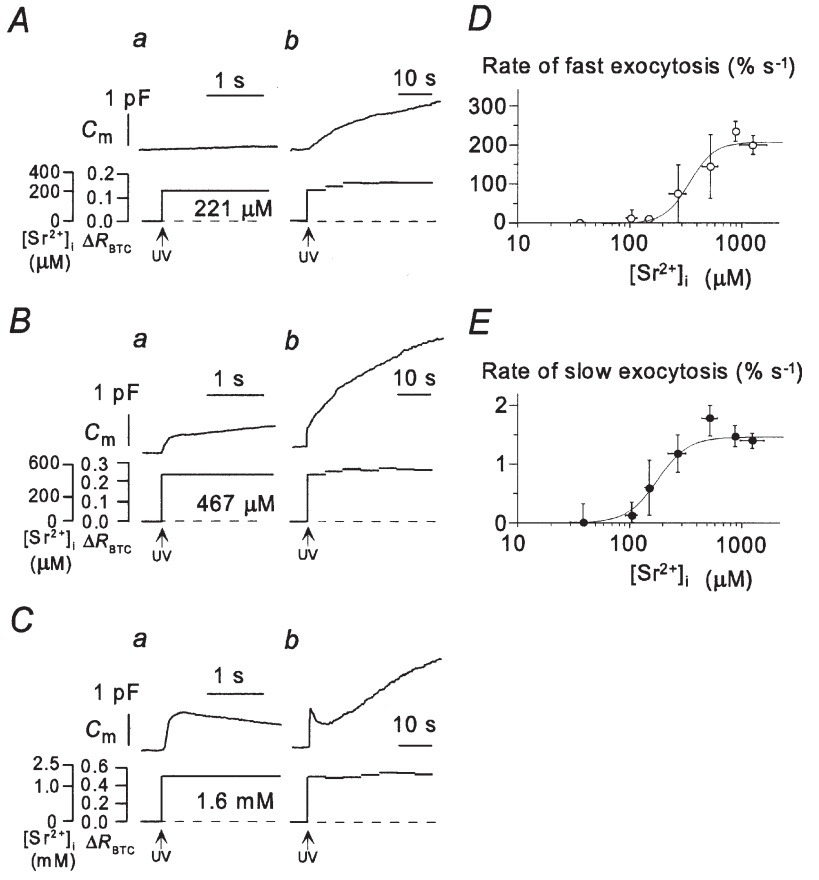

Figure 3. Sr^{2+}-induced exocytosis

A–C, representative experiments showing the two components of Sr^{2+}-dependent exocytosis in three different PC12 cells. Changes in C_m as well as in $[Sr^{2+}]_i$ and ΔR for BTC are shown in the upper and lower traces, respectively. The time axis in traces *a* is expanded by a factor of > 20 relative to that in traces *b*. *D* and *E*, dependence on $[Sr^{2+}]_i$ of the peak rates of the fast and slow components of exocytosis, respectively. Each point is the mean value from 4–15 experiments performed with different cells and with pipette solutions containing DM-nitrophen loaded with various amounts of $SrCl_2$.

In contrast, Sr^{2+} induced both the slow and the fast components of the increase in C_m. The slow component was apparent at $[Sr^{2+}]_i$ values of > 50 μM and its rate was half-maximal at 180 μM and maximal (1.5 ± 0.1 % s^{-1}) at > 300 μM (Fig. 3*A–C* and *E*). The fast component of exocytosis occurred at $[Sr^{2+}]_i$ values of > 150 μM and its rate was half-maximal at 320 μM and maximal at > 800 μM (Fig. 3*A–D*). The maximal rates of Sr^{2+}-induced LV and SV exocytosis were the same as those for Ca^{2+}-induced exocytosis (Figs 1*F* and *G*, 3*D* and *E*).

Sensitivities of the two components of exocytosis to Cd^{2+}, Mn^{2+}, Co^{2+} and Mg^{2+}

To characterize further the ion selectivities of the Ca^{2+} sensors for exocytosis in PC12 cells, we examined the effects of Mg^{2+}, Co^{2+}, Mn^{2+} and Cd^{2+} on the two components of this process. The slow component of exocytosis was induced by each of the four metal ions examined (Fig. 4*A–D*). It was apparent at cytosolic Cd^{2+} concentrations in the low picomolar range, at 150 nM Mn^{2+} and at 200 nM Co^{2+}, with half-maximal rates achieved at 18 pM Cd^{2+}, 500 nM Mn^{2+} and 900 nM Co^{2+} (Fig. 4*F*); it was induced even by Mg^{2+} at 6 mM (Fig. 4*D*). The maximal rates of Cd^{2+}-, Mn^{2+}- and Co^{2+}-induced LV exocytosis were the same as that of Ca^{2+}-induced LV exocytosis. In contrast, the fast component of exocytosis was induced substantially by Cd^{2+} and Mn^{2+}, but to only a small extent by Co^{2+} and not at all by Mg^{2+} (Fig. 4*A–D*). The fast component was detected at 10 pM Cd^{2+} and 100 nM Mn^{2+}, with the half-maximal rates apparent at 26 pM Cd^{2+} and 620 nM Mn^{2+} (Fig. 4*E*). The maximal rate of the fast component of Cd^{2+}-induced exocytosis was smaller than that of the corresponding value for Ca^{2+}-induced exocytosis, indicating that Cd^{2+} induces synchronous SV exocytosis less efficiently than does Ca^{2+}. The maximal rates of the fast components of Mn^{2+}- and Co^{2+}-induced exocytosis were also smaller than that of the corresponding value for Ca^{2+}-induced exocytosis. However, these differences might be due to the slow increases in the concentrations of these divalent cations that result from

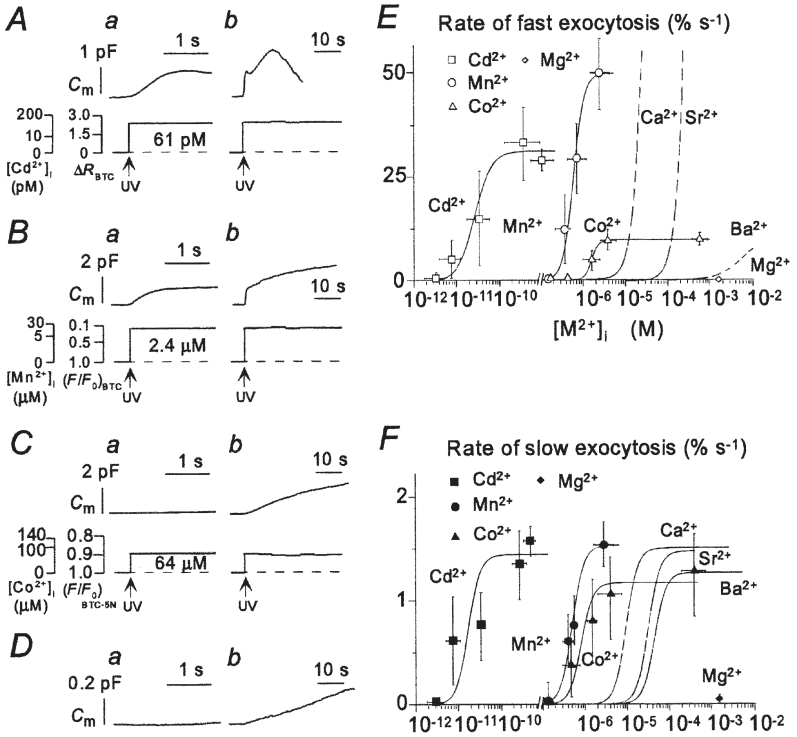

Figure 4. Heavy metal cation-induced exocytosis

A–D, components of exocytosis induced by rapid increases in the cytosolic concentrations of Cd^{2+}, Mn^{2+}, Co^{2+} or Mg^{2+}, respectively, in four different PC12 cells. Changes in C_m and the time courses of the cytosolic concentrations of the heavy metal cations (as well as ΔR for BTC and F/F_0 for BTC or BTC-5N, as indicated) are shown in the upper and lower traces, respectively. The time axis in traces *a* is expanded by a factor of > 20 relative to that in traces *b*. *E* and *F*, dependence of the peak rates of the fast (*E*) and slow (*F*) components of exocytosis on $[Cd^{2+}]_i$, $[Mn^{2+}]_i$ and $[Co^{2+}]_i$. Each point is the mean value from 3–8 experiments performed with different cells and with pipette solutions containing DM-nitrophen or DMNPE-4 loaded with various amounts of cation. Curves for Ca^{2+}, Sr^{2+} and Ba^{2+} are also included for comparison.

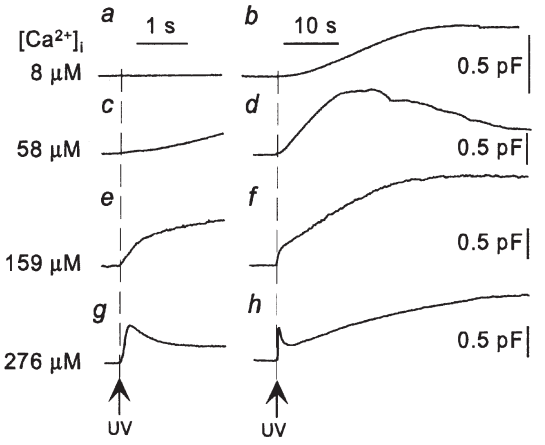

Figure 5. Competitive inhibition of the fast component of exocytosis by Na^+

Increases in $[Ca^{2+}]_i$ to the indicated values were induced in four different PC12 cells with an internal solution containing 155 mM Na^+ (Sol-Na). Each pair of left (*a*, *c*, *e* and *g*) and right (*b*, *d*, *f* and *h*) traces is from the same cell, but the time axis is expanded by a factor of > 20 in the left traces.

the long UV irradiation time required for the photolysis of caged-Ca^{2+} compounds complexed with Mn^{2+} or Co^{2+} (see Methods).

Inhibition of the fast component of exocytosis by Na^+

We noticed that the fast component of exocytosis was inhibited when all Cs^+ (115 mM) in the internal solution was replaced with Na^+; the fast component of exocytosis was small even at a $[Ca^{2+}]_i$ of 58 μM (Fig. 5*c*). This Na^+ block of the fast component of exocytosis was competitive, given that the size of this component increased to control values at a $[Ca^{2+}]_i$ of > 60 μM (Fig. 5*e* and *g*); the half-maximal rate was achieved at a $[Ca^{2+}]_i$ of 70 μM (Figs 5 and 6*B*). Thus, an increase in the concentration of Na^+ from 40 to 155 mM shifted the Ca^{2+} concentration for the half-maximal rate of the fast component of exocytosis by 46 μM. The results yield values of 14 μM and 44 mM for the macroscopic dissociation constants of the Ca^{2+} sensor for Ca^{2+} and Na^+, respectively, assuming a Hill coefficient of 3 for both Ca^{2+} and Na^+ binding. A Hill coefficient of 3 is necessary to account for the steep $[Na^+]_i$ dependence of the blocking action. This inhibitory effect was specific to Na^+ (Fig. 6*A*). The half-maximal rates for the fast component of exocytosis were apparent at a $[Ca^{2+}]_i$ of ~20–30 μM with internal solutions containing Li^+, K^+ or Cs^+ at 115 mM (Fig. 6*B*). The slow component of exocytosis was not blocked by any of the monovalent cations examined (Figs 5 and 6*A*).

DISCUSSION

We have systematically examined the ion selectivities of exocytosis by directly increasing the cytosolic concentrations of various divalent cations with the use of

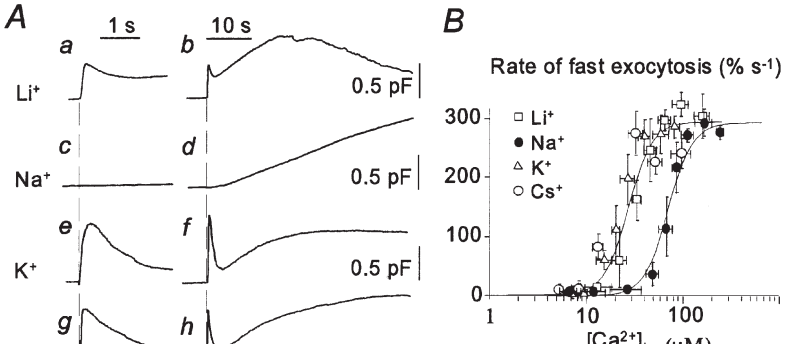

Figure 6. Ion selectivity of monovalent cation-induced inhibition of the fast component of exocytosis

A, two components of Ca^{2+}-dependent exocytosis were recorded from four different PC12 cells with internal solutions containing 115 mM Li^+ (traces *a* and *b*), 155 mM Na^+ (traces *c* and *d*), 115 mM K^+ (traces *e* and *f*) or 115 mM Cs^+ (traces *g* and *h*); the induced increases in $[Ca^{2+}]_i$ were 42, 32, 35 and 50 μM, respectively. Each pair of left (*a*, *c*, *e* and *g*) and right (*b*, *d*, *f* and *h*) traces is from the same cell, but the time axis is expanded by a factor of > 20 in the left traces. *B*, dependence on $[Ca^{2+}]_i$ of the peak rate of the fast component of exocytosis. Each point is a mean value from 3–6 experiments performed with different cells and with pipette solutions containing the indicated monovalent cations as well as DM-nitrophen loaded with various amounts of $CaCl_2$.

caged-Ca^{2+} compounds. Our results indicate that the two components of exocytosis in PC12 cells exhibit distinct ion selectivities. They thus provide a new line of evidence for the hypothesis that the two components of exocytosis are mediated by two distinct types of secretory vesicle, SVs and LVs, in PC12 cells (Kasai, 1999). Our data are not inconsistent with a model that assumes transitions of state within a single population of vesicles in adrenal chromaffin cells (Gillis *et al.* 1996; Smith *et al.* 1998; Voets, 2000), given that, unlike in PC12 cells (Ninomiya *et al.* 1997), the major component of exocytosis is attributed to LVs in chromaffin cells (Haller *et al.* 1998; Kasai, 1999).

The slow component of exocytosis in PC12 cells, representing LV exocytosis, was induced by all divalent metal ions investigated, with half-maximal rates apparent at cytosolic concentrations of 18 pM for Cd^{2+}, 500 nM for Mn^{2+}, 900 nM for Co^{2+}, 8 μM for Ca^{2+}, 180 μM for Sr^{2+} and 280 μM for Ba^{2+}. The extent of synaptotagmin–phospholipid binding is half-maximal at Ca^{2+}, Sr^{2+} and Ba^{2+} concentrations of 5.4, 177 and 254 μM, respectively (Li *et al.* 1995), values that are similar to those that give rise to half-maximal rates for the slow component of exocytosis in PC12 cells. In addition, exocytosis of LVs in endocrine cells monitored either biochemically (Berggren, 1981; Douglas *et al.* 1983; Brown *et al.* 1990), by capacitance measurement (Seward *et al.* 1996; Nucifora & Fox, 1998) or by amperometry (von Ruden *et al.* 1993; Borges *et al.* 1997) has been shown to be supported by Ba^{2+} in place of Ca^{2+} in the external solution. Thus, the ion selectivity of the slow component of exocytosis quantified in the present study supports a major role for synaptotagmin–phospholipid in the triggering of exocytosis of LVs.

The fast component of exocytosis in PC12 cells, representing synchronous SV exocytosis, appeared more selective for divalent cations than did the slow component. The rate of the fast component was half-maximal at 26 pM Cd^{2+}, 620 nM Mn^{2+}, 24 μM Ca^{2+} and 320 μM Sr^{2+}, and this component was little activated by Ba^{2+} (< 1 mM) or Co^{2+}. Moreover, the fast component of exocytosis was competitively inhibited by high concentrations of Na^+ but not by K^+, Li^+ or Cs^+. This pattern of ion selectivity can be explained by the ionic radii of these cations, given that the divalent cations (Mn^{2+}, Cd^{2+} and Sr^{2+}) and monovalent cation (Na^+) with radii most similar to that of Ca^{2+} triggered and inhibited, respectively, the fast component of exocytosis (Fig. 7). A similar divalent ion selectivity is exhibited by EF-hand proteins such as calmodulin (Chao *et al.* 1984). The binding of Ca^{2+} to the EF-hand proteins α-lactalbumin (Eberhard & Erne, 1991) and parvalbumin (Permyakov *et al.* 1983; Eberhard & Erne, 1994) is also inhibited by Na^+. Previous studies have shown that synchronous synaptic transmission is maintained when external Ca^{2+} is replaced by Sr^{2+}, but is supported to only a small extent, or not at all, by external Ba^{2+} (Dodge *et al.* 1969; Alvarez-Leefmans *et al.* 1978; Augustine & Eckert, 1984; Medina *et al.* 1994; Ohno-Shosaku *et al.* 1994). Thus, the ion selectivity of both synchronous synaptic transmission and the fast component of exocytosis in PC12 cells is more stringent than that of exocytosis of LVs.

There is some uncertainty as to whether the fast component of the capacitance increase faithfully reflects the exocytosis of SVs. First, this component may also reflect changes in other electrical properties of the plasma membrane caused by a sudden increase in $[Ca^{2+}]_i$. However, the complete absence of the fast component of the capacitance increase in PC12 cells exposed to Ba^{2+} (< 1 mM) or Co^{2+} jumps or to Ca^{2+} jumps (< 58 μM) in the presence of 155 mM Na^+ is consistent with the conclusion that fast synchronous SV exocytosis is not induced by Ba^{2+} (< 1 mM) or Co^{2+} and is blocked by Na^+. Second, the fast component of the capacitance increase may be curtailed by concurrent endocytosis even at the peak of the increase that is apparent within 0.2 s. However, endocytosis occurs only in the presence of exocytosis and the ion selectivities of each component of the capacitance increase in PC12 cells were identical when measured at the minimal effective concentrations or the median effective concentrations (Fig. 4*E* and *F*).

The ion selectivity of synchronous SV exocytosis in PC12 cells appears inconsistent with that of the synaptotagmin–phospholipid interaction. The more stringent ion selectivity and higher $[Ca^{2+}]_i$ requirement of synchronous SV exocytosis suggests a larger coordination number and smaller negative charge for the Ca^{2+} binding

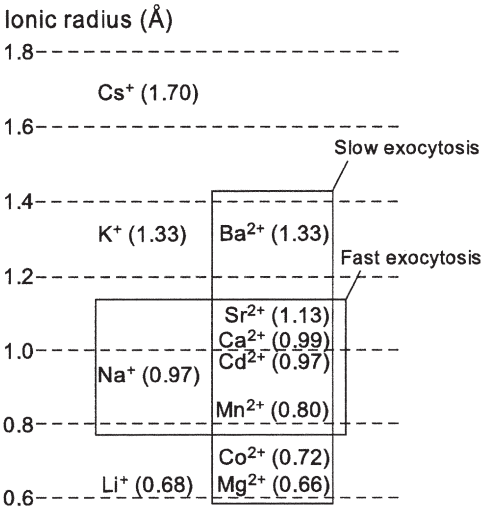

Figure 7. Ionic radii and ion selectivities of exocytosis in PC12 cells

The exocytosis of LVs was induced by all divalent cations studied, whereas synchronous SV exocytosis was induced by the divalent cations with ionic radii most similar to that of Ca^{2+} and was blocked selectively by Na^+. 1 Å = 0.1 nm.

sites that underlie synchronous SV exocytosis. Such Ca^{2+} binding sites may be provided by (1) the synaptotagmin–phospholipid interaction in a distinct conformational state (Davis *et al.* 1999), (2) the interaction of synaptotagmin with syntaxin (Li *et al.* 1995) or SNAP25 (Gerona *et al.* 2000), or (3) another Ca^{2+} binding protein with a high ion selectivity, such as an EF-hand protein (Peters & Mayer, 1998; Quetglas *et al.* 2000). Testing the actions of Ba^{2+} and Na^{+} in the experiments cited above (Li *et al.* 1995; Peters & Mayer, 1998; Davis *et al.* 1999; Quetglas *et al.* 2000; Gerona *et al.* 2000) may help to clarify the molecular events that underlie synchronous SV exocytosis.

Alvarez-Leefmans, F. J., De Santis, A. & Miledi, R. (1978). Effects of removal of calcium and its replacement by strontium and barium ions on synaptic transmission in frog spinal neurons. *Journal of Physiology* **278**, 10–11*P*.

Augustine, G. J. & Charlton, M. P. (1986). Calcium dependence of presynaptic calcium current and post-synaptic response at the squid giant synapse. *Journal of Physiology* **381**, 619–640.

Augustine, G. J. & Eckert, R. (1984). Divalent cations differentially support transmitter release at the squid giant synapse. *Journal of Physiology* **346**, 257–271.

Baumert, M., Takei, K., Hartinger, J., Burger, P. M., Fischer, V. M., Maycox, P. R., De Camilli, P. & Jahn, R. (1990). P29: a novel tyrosine-phosphorylated membrane protein present in small clear vesicles of neurons and endocrine cells. *Journal of Cell Biology* **110**, 1285–1294.

Berggren, P. O. (1981). Characteristics of Ba^{2+}-stimulated insulin release with special reference to pancreatic β-cells sensitized by cyclic AMP. *Acta Biologica et Medica Germanica* **40**, 15–17.

Bollmann, J. H., Sakmann, B. & Borst, J. G. (2000). Calcium sensitivity of glutamate release in a calyx-type terminal. *Science* **289**, 953–957.

Bommert, K., Charlton, M. P., Debello, W. M., Chin, G. J., Betz, H. & Augustine, G. J. (1993). Inhibition of neurotransmitter release by C2-domain peptides implicates synaptotagmin in exocytosis. *Nature* **363**, 163–165.

Borges, R., Travis, E. R., Hochstetler, S. E. & Wightman, R. M. (1997). Effects of external osmotic pressure on vesicular secretion from bovine adrenal medullary cells. *Journal of Biological Chemistry* **272**, 8325–8331.

Brose, N., Petrenko, A. G., Südhof, T. C. & Jahn, R. (1992). Synaptotagmin: a calcium sensor on the synaptic vesicle surface. *Science* **256**, 1021–1025.

Brown, E. M., Fuleihan, G. E., Chen, C. J. & Kifor, O. (1990). A comparison of the effects of divalent and trivalent cations on parathyroid hormone release, 3′,5′-cyclic-adenosine monophosphate accumulation and the levels of inositol phosphates in bovine parathyroid cells. *Endocrinology* **127**, 1064–1071.

Chao, S. H., Suzuki, Y., Zysk, J. R. & Cheung, W. Y. (1984). Activation of calmodulin by various metal cations as a function of ionic radius. *Molecular Pharmacology* **26**, 75–82.

Clift, O. G., Linstedt, A. D., Lowe, A. W., Grote, E. & Kelly, R. B. (1990). Biogenesis of synaptic vesicle-like structures in a pheochromocytoma cell line PC-12. *Journal of Cell Biology* **110**, 1693–1703.

Davis, A. F., Bai, J., Fasshauer, D., Wolowick, M. J., Lewis, J. L. & Chapman, E. R. (1999). Kinetics of synaptotagmin responses to Ca^{2+} and assembly with the core SNARE complex onto membranes. *Neuron* **24**, 363–376.

Delaney, K. R. & Zucker, R. S. (1990). Calcium released by photolysis of DM-nitrophen stimulates transmitter release at squid giant synapse. *Journal of Physiology* **426**, 473–498.

Dodge, F. A. J., Miledi, R. & Rahamimoff, R. (1969). Strontium and quantal release of transmitter at the neuromuscular junction. *Journal of Physiology* **200**, 267–283.

Dodge, F. A. J. & Rahamimoff, R. (1967). Co-operative action of calcium ions in transmitter release at the neuromuscular junction. *Journal of Physiology* **193**, 419–432.

Douglas, W. W., Taraskevich, P. S. & Tomiko, S. A. (1983). Secretagogue effect of barium on output of melanocyte-stimulating hormone from pars intermedia of the mouse pituitary. *Journal of Physiology* **338**, 243–257.

Eberhard, M. & Erne, P. (1991). Analysis of calcium binding to α-lactalbumin using a fluorescent calcium indicator. *European Journal of Biochemistry* **202**, 1333–1338.

Eberhard, M. & Erne, P. (1994). Calcium and magnesium binding to rat parvalbumin. *European Journal of Biochemistry* **222**, 21–26.

Elferink, L. A., Peterson, M. R. & Scheller, R. H. (1993). A role for synaptotagmin (p65) in regulated exocytosis. *Cell* **72**, 153–159.

Ellis-Davies, G. C. (1998). Synthesis of photosensitive EGTA derivatives. *Tetrahedron Letters* **39**, 953–956.

Gerona, R. R., Larsen, E. C., Kowalchyk, J. A. & Martin, T. F. (2000). The C terminus of SNAP25 is essential for Ca^{2+}-dependent binding of synaptotagmin to SNARE complexes. *Journal of Biological Chemistry* **275**, 6328–6336.

Gillis, K. D., Moesner, R. & Neher, E. (1996). Protein kinase C enhances exocytosis from chromaffin cells by increasing the size of the readily releasable pool of secretory granules. *Neuron* **16**, 1209–1220.

Greene, L. A. & Tischler, A. S. (1976). Establishment of a noradrenergic clonal line of rat adrenal pheochromocytoma cells which respond to nerve growth factor. *Proceedings of the National Academy of Sciences of the USA* **73**, 2424–2428.

Grynkiewicz, G., Poenie, M. & Tsien, R. Y. (1985). A new generation of Ca^{2+} indicators with greatly improved fluorescence properties. *Journal of Biological Chemistry* **260**, 3440–3450.

Haller, M., Heinemann, C., Chow, R. H., Heidelberger, R. & Neher, E. (1998). Comparison of secretory responses as measured by membrane capacitance and by amperometry. *Biophysical Journal* **74**, 2100–2113.

Itakura, M., Misawa, H., Sekiguchi, M., Takahashi, S. & Takahashi, M. (1999). Transfection analysis of functional roles of complexin I and II in the exocytosis of two different types of secretory vesicles. *Biochemical and Biophysical Research Communications* **265**, 691–696.

Kasai, H. (1999). Comparative biology of Ca^{2+}-dependent exocytosis: implications of kinetic diversity for secretory function. *Trends in Neurosciences* **22**, 88–93.

Kasai, H., Kishimoto, T., Liu, T. T., Miyashita, Y., Podini, P., Grohovaz, F. & Meldolesi, J. (1999). Multiple and diverse forms of regulated exocytosis in wild-type and defective PC12 cells. *Proceedings of the National Academy of Sciences of the USA* **96**, 945–949.

Kasai, H., Takagi, H., Ninomiya, Y., Kishimoto, T., Ito, K., Yoshida, A., Yoshioka, T. & Miyashita, Y. (1996). Two components of exocytosis and endocytosis in phaeochromocytoma cells studied using caged Ca^{2+} compounds. *Journal of Physiology* **494**, 53–65.

Kelly, R. B. (1993). Storage and release of neurotransmitters. *Cell* **72**, 43–53.

Knight, D. E. & Baker, P. F. (1982) Calcium-dependence of catecholamine release from bovine adrenal medullary cells after exposure to intense electric fields. *Journal of Membrane Biology* **68**, 107–140.

Li, C., Davletov, B. A. & Südhof, T. C. (1995). Distinct Ca^{2+} and Sr^{2+} binding properties of synaptotagmins. Definition of candidate Ca^{2+} sensors for the fast and slow components of neurotransmitter release. *Journal of Biological Chemistry* **270**, 24898–24902.

McMahon, H. T. & Nicholls, D. G. (1993). Barium-evoked glutamate release from guinea-pig cerebrocortical synaptosomes. *Journal of Neurochemistry* **61**, 110–115.

Maeda, H., Ellis-Davies, G. C., Ito, K., Miyashita, Y. & Kasai, H. (1999). Supralinear Ca^{2+} signaling by cooperative and mobile Ca^{2+} buffering in Purkinje neurons. *Neuron* **24**, 989–1002.

Martell, A. E. & Smith, R. M. (1974). *Critical Stability Constants*. Plenum, New York.

Medina, J. I., Barden, S. D., Davies, M. S., Newell, B. A., Shaw, S. A., Willis, M. & Halliwell, J. V. (1994). Barium ions fail to support neurotransmission at a central synapse. *Neuroscience Letters* **168**, 106–110.

Mikoshiba, K., Fukuda, M., Ibata, K., Kabayama, H. & Mizutani, A. (1999). Role of synaptotagmin, a Ca^{2+} and inositol polyphosphate binding protein, in neurotransmitter release and neurite outgrowth. *Chemistry and Physics of Lipids* **98**, 59–67.

Ninomiya, Y., Kishimoto, T., Yamazawa, T., Ikeda, H., Miyashita, Y. & Kasai, H. (1997). Kinetic diversity in the fusion of exocytotic vesicles. *EMBO Journal* **16**, 929–934.

Nucifora, P. G. & Fox, A. P. (1998). Barium triggers rapid endocytosis in calf adrenal chromaffin cells. *Journal of Physiology* **508**, 483–494.

Ohno-Shosaku, T., Sawada, S., Hirata, K. & Yamamoto, C. (1994). A comparison between potencies of external calcium, strontium and barium to support GABAergic synaptic transmission in rat cultured hippocampal neurons. *Neuroscience Research* **20**, 223–229.

Permyakov, E. A., Kalinichenko, L. P., Medvedkin, V. N., Burstein, E. A. & Gerday, C. (1983). Sodium and potassium binding to parvalbumins measured by means of intrinsic protein fluorescence. *Biochimica et Biophysica Acta* **749**, 185–191.

Peters, C. & Mayer, A. (1998). Ca^{2+}/calmodulin signals the completion of docking and triggers a late step of vacuole fusion. *Nature* **396**, 575–580.

Quetglas, S., Leveque, C., Miquelis, R., Sato, K. & Seagar, M. (2000). Ca^{2+}-dependent regulation of synaptic SNARE complex assembly via a calmodulin- and phospholipid-binding domain of synaptobrevin. *Proceedings of the National Academy of Sciences of the USA* **97**, 9695–9700.

Schmidt, A., Hannah, M. J. & Huttner, W. B. (1997). Synaptic-like microvesicles of neuroendocrine cells originate from a novel compartment that is continuous with the plasma membrane and devoid of transferrin receptor. *Journal of Cell Biology* **137**, 445–458.

Schneggenburger, R. & Neher, E. (2000). Intracellular calcium dependence of transmitter release rates at a fast central synapse. *Nature* **406**, 889–893.

Seward, E. P., Chernevskaya, N. I. & Nowycky, M. C. (1996). Ba^{2+} ions evoke two kinetically distinct patterns of exocytosis in chromaffin cells, but not in neurohypophysial nerve terminals. *Journal of Neuroscience* **16**, 1370–1379.

Sihra, T. S., Piomelli, D. & Nichols, R. A. (1993). Barium evokes glutamate release from rat brain synaptosomes by membrane depolarization: involvement of K^+, Na^+ and Ca^{2+} channels. *Journal of Neurochemistry* **61**, 1220–1230.

Silinsky, E. M. (1978). On the role of barium in supporting the asynchronous release of acetylcholine quanta by motor nerve impulses. *Journal of Physiology* **274**, 157–171.

Smith, C., Moser, T., Xu, T. & Neher, E. (1998). Cytosolic Ca^{2+} acts by two separate pathways to modulate the supply of release-competent vesicles in chromaffin cells. *Neuron* **20**, 1245–1253.

Smith, C. B. & Betz, W. J. (1996). Simultaneous independent measurement of endocytosis and exocytosis. *Nature* **380**, 531–534.

Südhof, T. C. & Rizo, J. (1996). Synaptotagmins: C2-domain proteins that regulate membrane traffic. *Neuron* **17**, 379–388.

Takahashi, N., Kadowaki, T., Yazaki, Y., Miyashita, Y. & Kasai, H. (1997). Multiple exocytotic pathways in pancreatic β cells. *Journal of Cell Biology* **138**, 55–64.

Takahashi, T. & Momiyama, A. (1993). Different types of calcium channels mediate central synaptic transmission. *Nature* **366**, 156–158.

Thomas, D. M. & Elferink, L. A. (1998). Functional analysis of the C2A domain of synaptotagmin 1: implications for calcium-regulated secretion. *Journal of Neuroscience* **18**, 3511–3520.

Tomsig, J. L. & Suszkiw, J. B. (1996). Metal selectivity of exocytosis in α-toxin-permeabilized bovine chromaffin cells. *Journal of Neurochemistry* **66**, 644–650.

Verhage, M., Hens, J. J., De Grann, P. N., Boomsma, F., Wiegant, V. M., Da Silva, F. H., Gispen, W. H. & Ghijsen, W. E. (1995). Ba^{2+} replaces Ca^{2+}/calmodulin in the activation of protein phosphatases and in exocytosis of all major transmitters. *European Journal of Pharmacology* **291**, 387–398.

Voets, T. (2000). Dissection of three Ca^{2+}-dependent steps leading to secretion in chromaffin cells from mouse adrenal slices. *Neuron* **28**, 537–545.

Von Ruden, L., Garcia, A. G. & Lopez, M. G. (1993). The mechanism of Ba^{2+}-induced exocytosis from single chromaffin cells. *FEBS Letters* **336**, 48–52.

Acknowledgements

We thank K. Inoue for providing a clone of PC12 cells and M. Osaka and M. Ogawa for technical assistance. This work was supported by the Research for the Future program of the Japan Society for the Promotion of Science (JSPS); CREST (Core Research for Evolutional Science and Technology) of the Japan Science and Technology Corporation (JST); Grants-in-Aid from the Japanese Ministry of Education, Culture, Sports, Science and Technology; and NIH (GM53395).

Corresponding author

T. Kishimoto: Department of Cell Physiology, National Institute for Physiological Sciences, Okazaki 444-8585, Japan.

Email: takuya@nips.ac.jp